Finite Volume Meshless Local Petrov-Galerkin Method in Vibration of Structures

Mohammad Moosavi, Abdel Khelil

Finite Volume Meshless Local Petrov-Galerkin Method in Vibration of Structures

M.R. Moosavi, A. Khelil

Nancy Université, LEMTA CNRS UMR 7563
IUT Nancy Brabois Génie Civil – 54601 Villers Les Nancy cedex

{Mohammad-reza.moosavi, abdel.khelil}@iutnb.uhp-nancy.fr

Abstract – A Finite Volume Meshless Local Petrov-Galerkin (FVMLPG) method is presented for elastodynamic problems. It is derived from the local weak form of the equilibrium equations by using the Finite Volume (FV) and the Meshless Local Petrov-Galerkin (MLPG) concepts. By incorporating the moving least squares (MLS) approximations for trial functions, the local weak form is discretized, and is integrated over the local subdomain. Numerical examples for solving the transient response of the elastic structures are included.

Key words – Finite Volume (FV), Meshless Local Petrov-Galerkin (MLPG), Structural Transient Analysis

1 Introduction

The meshless local Petrov-Galerkin approach [1], based on the local symmetric weak form (LSWF) and the moving least squares (MLS) approximation, is a truly numerical meshless method for solving boundary value problems. The primary advantage of this method over the extensively used mesh based method and other so-called meshless methods such as the diffuse element method [2], the element free Galerkin method [3], and the reproducing kernel particle method [4], is that it does not require a finite element mesh, either to interpolate the solution variables, or to integrate the energy. Recently, a meshless local boundary integral equation method [5] with the Houbolt finite difference scheme was successfully applied to solve 2D elastodynamic problems.

The Finite Volume Meshless Local Petrov-Galerkin (FVMLPG) method [6] is a new meshless method for the discretization of conservation laws. The motivation for developing a new method is to unify advantages of meshless methods and Finite Volume Methods (FVM) in one scheme. Meshless methods are very flexible because they do not require using any mesh. The need for meshless methods will typically arise if problems with time dependent or very complicated geometries are under consideration because then the grid handling become technically complicated or very time consuming. The basic idea of the FVMLPG is to incorporate elements of Finite Volume methods into Meshless Local Petrov-Galerkin (MLPG) method. In this present study, the FVMLPG approach for solving problems in elastodynamics is developed. The method utilizes a local symmetric weak form (LSWF) and shape functions from the MLS approximation. In the present formulation, a generalized local weak form of the governing differential equation is represented by the finite volume method (FVM). The trial functions are approximated by the MLS approximation. The FVMLPG method for solving problems in elastodynamics is a truly meshless method, and needs absolutely no meshes of either the traditional mesh based type, either to interpolate the solution variables, or to integrate the energy. The formulation involves only domain and boundary integrals over very regular

subdomains and their boundaries. These integrals can be easily and directly evaluated over the very regular shapes of the subdomains and their boundaries.

2 Finite Volume Meshless Local Petrov-Galerkin Method

A generalized local weak form of the differential equation over a local sub-domain Ω_s, can be written as

$$\int_{\Omega_s} \left(\sigma_{ij,j} + f_i - \rho\ddot{u}_i\right) v_i \, \mathrm{d}\Omega = 0 \,. \tag{1}$$

Bc's: $u_i = \overline{u}_i$ on Γ_u, $\overline{u}_i$: prescribed displacements, Γ_u: displacements boundary (2)

$t_i = \sigma_{ij} n_j = \overline{t}_i$ on Γ_t, $\overline{t}_i$: prescribed tractions, n_j: Γ_t: traction boundary (3)

Imposing the boundary conditions Eq. (2) and (3) in Eq. (1), one obtains

$$\int_{L_s} t_i v_i d\Gamma + \int_{\Gamma_{su}} t_i v_i d\Gamma + \int_{\Gamma_{st}} \overline{t}_i v_i d\Gamma - \int_{\Omega_s} \left(\sigma_{ij} v_{i,j} - f_i v_i - \rho\ddot{u}_i v_i\right) d\Omega = 0 \tag{4}$$

In Eq. (4), there are two sets of local boundaries; one is the boundary which is completely inside of the global domain, shown by L_s; the other one is the boundary which has a common side with the boundary of the global domain, indicated by Γ_s. If the common part is on the displacement boundary Γ_u, it is called Γ_{su}, in other words, $\Gamma_{su} = \Gamma_s \bigcap \Gamma_u$; and if the shared part is on the traction boundary Γ_t it is named Γ_{st} or in other words, $\Gamma_{st} = \Gamma_s \bigcap \Gamma_t$. Therefore, a local symmetric weak form (LSWF) in linear elastodynamics can be written as

$$\int_{\Omega_s} \sigma_{ij} v_{i,j} d\Omega - \int_{L_s} t_i v_i d\Gamma - \int_{\Gamma_{su}} t_i v_i d\Gamma + \int_{\Omega_s} \rho\ddot{u}_i v_i d\Omega = \int_{\Gamma_{st}} \overline{t}_i v_i d\Gamma + \int_{\Omega_s} f_i v_i d\Omega \tag{5}$$

With the constitutive relations of an isotropic linear elastic homogeneous solid, the tractions in Eq. (5) can be written in term of the strains

$$\int_{\Omega_s} \rho\ddot{u}_i d\Omega - \int_{L_s} E_{ijkl}\varepsilon_{kl} n_j d\Gamma - \int_{\Gamma_{su}} E_{ijkl}\varepsilon_{kl} n_j d\Gamma = \int_{\Gamma_{st}} \overline{t}_i d\Gamma + \int_{\Omega_s} f_i d\Omega \tag{6}$$

In Eq. (6), displacement and strain are approximated as

$$u_i(\mathrm{x},t) = \sum_{J=1}^{n} \Phi^{(J)}(\mathrm{x}) u_i^{(J)}(t) \qquad \varepsilon_{kl}(\mathrm{x},t) = \sum_{K=1}^{n} \Phi^{(K)}(\mathrm{x}) \varepsilon_{kl}^{(K)}(t) \tag{7}$$

where $\Phi^{(J)}(\mathrm{x})$ and $\Phi^{(K)}(\mathrm{x})$ are the shape functions, $u_i^{(J)}$ and $\varepsilon_{kl}^{(K)}$ are displacement and strain in node I, respectively. By substituting Eq. (7) in Eq. (6), this equation can be discretized as

$$\begin{aligned} &\sum_{J=1}^{n}\left[\int_{\Omega_s} \Phi^{(J)}(\mathrm{x}) \rho d\Omega\right] \ddot{u}_i^{(J)}(t) - \sum_{K=1}^{n}\left[\int_{L_s} \Phi^{(K)}(\mathrm{x}) E_{ijkl} n_j d\Gamma\right] \varepsilon_{kl}^{(K)}(t) \\ &- \sum_{K=1}^{n}\left[\int_{\Gamma_{su}} \Phi^{(K)}(\mathrm{x}) E_{ijkl} n_j d\Gamma\right] \varepsilon_{kl}^{(K)}(t) = \int_{\Gamma_{st}} \overline{t}_i d\Gamma + \int_{\Omega_s} f_i d\Omega \end{aligned} \tag{8}$$

The advantage of Eq. (8) is that it does not contain any shape function derivative; because the meshless approximation is not efficient for calculating such derivative everywhere in the domain, especially when the MLS approximation is used. Hence, it is the benefit resulting from this work in comparison with the traditional MLPG [primal] displacement method; in other words, in the primal MLPG, the displacement is approximated directly, therefore the derivative of the shape function will appear in the discretized local form.

3 Time integration

The Newmark β method [7], well known and commonly applied in computations, is used in the present study to integrate the governing equations in time. The accelerations, the displacements and velocities are calculated from the standard Newmark β method, as

$$\begin{aligned} \mathrm{u}^{t+\Delta t} &= \mathrm{u}^{t} + \Delta t \mathrm{v}^{t} + \frac{\Delta t^2}{2}\left[\left(1-2\beta\right)\mathrm{a}^{t} + 2\beta \mathrm{a}^{t+\Delta t}\right] \\ \mathrm{v}_c^{t+\Delta t} &= \mathrm{v}^{t} + \Delta t\left[\left(1-\gamma\right)\mathrm{a}^{t} + \gamma \mathrm{a}^{t+\Delta t}\right] \end{aligned} \tag{9}$$

For zero damping system, this method is unconditionally stable if

$$2\beta \geq \gamma \geq \frac{1}{2} \tag{10}$$

and conditionally stable if

$$\gamma \geq \frac{1}{2},\ \beta \leq \frac{1}{2} \text{ and } \Delta t \leq \frac{1}{\omega_{\max}\sqrt{\gamma/2-\beta}} \tag{11}$$

where $\omega_{\max}$ is the maximum frequency in the structural system.

This method can be used in the predictor-corrector way. After specifying the initial conditions, the time integrations for each time increment can be done in the following steps.

Step 1: predict the displacements and velocities

$$\begin{aligned} \hat{\mathrm{u}}_c^{t+\Delta t} &= \hat{\mathrm{u}}^{t} + \Delta t \hat{\mathrm{v}}^{t} + \frac{\Delta t^2}{2}\left(1-2\beta\right)\hat{\mathrm{a}}^{t} \\ \hat{\mathrm{v}}_c^{t+\Delta t} &= \hat{\mathrm{v}}^{t} + \Delta t\left(1-\gamma\right)\hat{\mathrm{a}}^{t} \end{aligned} \tag{12}$$

Step 2: predict the acceleration

$$\begin{aligned} \hat{\mathrm{a}}_{c1}^{t+\Delta t} &= \mathrm{M}^{-1}\cdot\left(\hat{\mathrm{f}}^{t+\Delta t} - \mathrm{K}\cdot\hat{\mathrm{u}}_c^{t+\Delta t}\right) \\ \hat{\mathrm{a}}_{c2}^{t+\Delta t} &= \hat{\mathrm{a}}_{c1}^{t+\Delta t} - \mathrm{G}\cdot\mathrm{G}^{T}\cdot\hat{\mathrm{a}}_{c1}^{t+\Delta t} \end{aligned} \tag{13}$$

Step 3: correct the displacements and velocities

$$\begin{aligned} \hat{\mathrm{u}}^{t+\Delta t} &= \hat{\mathrm{u}}_c^{t+\Delta t} + \Delta t^2\beta\hat{\mathrm{a}}_{c2}^{t+\Delta t} \\ \hat{\mathrm{v}}^{t+\Delta t} &= \hat{\mathrm{v}}_c^{t+\Delta t} + \Delta t\gamma\hat{\mathrm{a}}_{c2}^{t+\Delta t} \end{aligned} \tag{14}$$

Step 4: correct the acceleration

$$\hat{\mathrm{a}}_{c3}^{t+\Delta t} = \mathrm{M}^{-1} \cdot \left(\hat{\mathrm{f}}^{t+\Delta t} - \mathrm{K} \cdot \hat{\mathrm{u}}^{t+\Delta t} \right)$$

$$\hat{\mathrm{a}}^{t+\Delta t} = \hat{\mathrm{a}}_{c3}^{t+\Delta t} - \mathrm{G} \cdot \mathrm{G}^{T} \cdot \hat{\mathrm{a}}_{c3}^{t+\Delta t}$$

6 Numerical example

A computer code is developed in Matlab for this numerical procedure. Consider a rod fixed rigidly at its base and subjected to a step-function loading f_0 at the upper end, as shown in Fig. 1. The exact solution at any time t can be obtained by Eqs. (14) and (15) representing the displacement and force distributions [8].

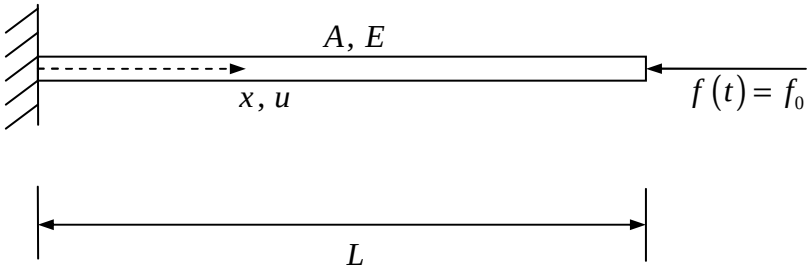

(a)

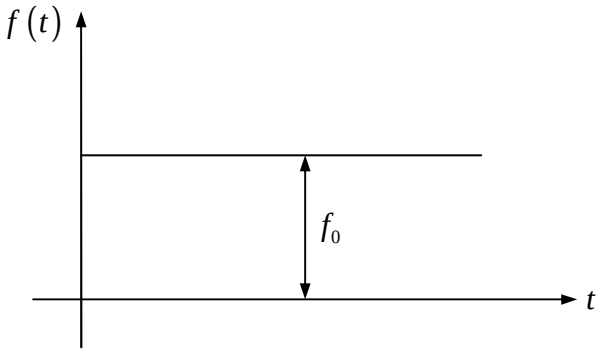

(b)

Figure 1 - Rod subjected to end loading: **(a)** geometric configuration; **(b)** step-function loading

$$u(x,t) = \frac{8 f_0}{\pi^2} \frac{L}{AE} \sum_{n=1}^{\infty} \left[(\pm) \frac{1-\cos \omega_n t}{(2n-1)^2} \sin \frac{2n-1}{2} \frac{\pi x}{L} \right] \tag{14}$$

$$F(x,t) = \frac{4 f_0}{\pi} \sum_{n=1}^{\infty} \left[(\pm) \frac{1-\cos \omega_n t}{2n-1} \cos \frac{2n-1}{2} \frac{\pi x}{L} \right] \tag{15}$$

When solving the problem by the FVMLPG method, we took $L=24$, $E=1$, $\rho=1$, $A=1$, and $f(t)=H(t)$ where $H(t)$ is the Heaviside step function. The bar was divided into 49 equally spaced nodes. The Newmark β method with the time step size, Δt, equaled $1.0\,\mu s$ is used in this example. The maximum frequency, $\omega_{\max}$, is 0.0654 Hz. The axial displacement and force along the rod are shown in Fig. 3. The results indicate a very good agreement between the FVMLPG and the exact solution.

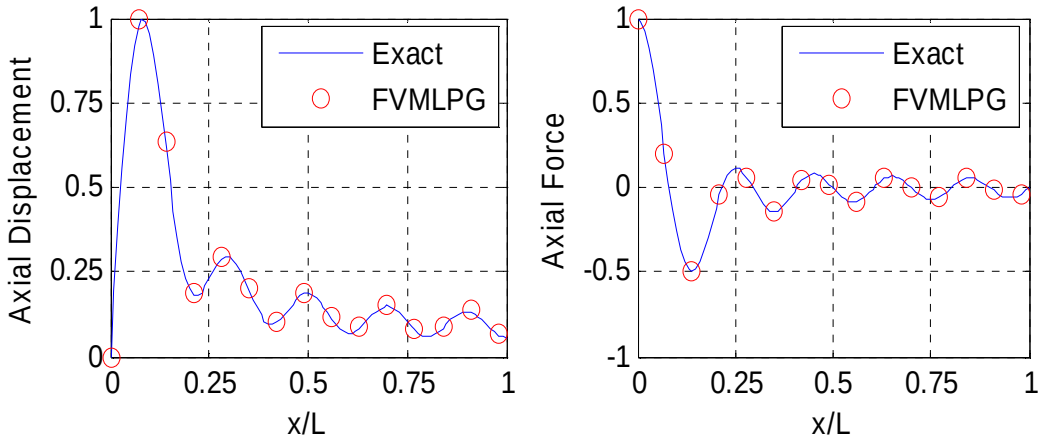

(a) t = 0.1 s

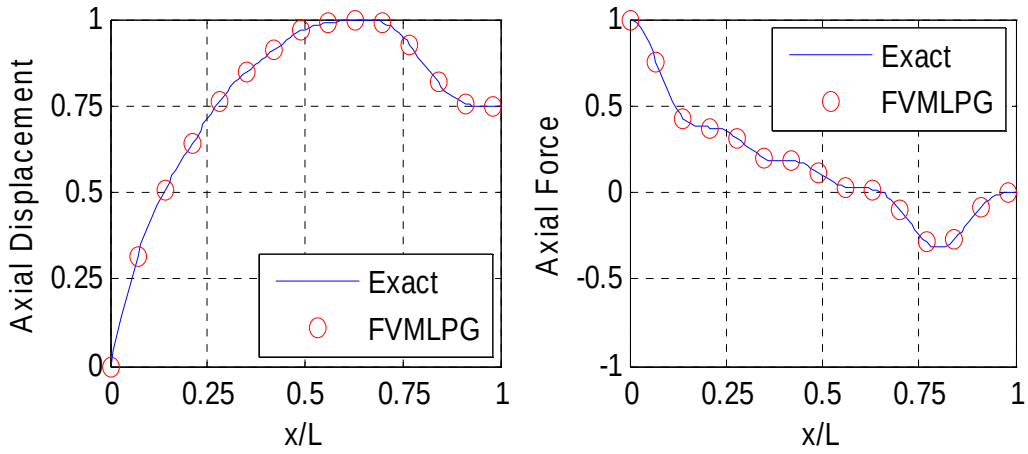

(b) t = 0.8 s

Figure 2 - Axial displacement and axial force of the rod

Figure 3 shows the comparison between the analytical solution of the time histories of the axial displacement and force at the midpoint (x = L/2) with the ones which computed with this scheme. It is clear the results of the FVMLPG in the axial displacement and force are very good in compare to the ones of the exact solutions.

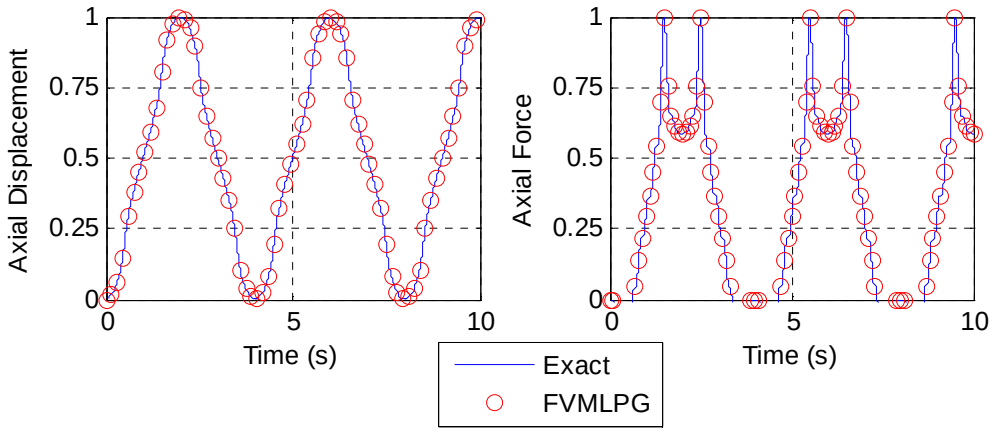

Figure 3 - Axial force time history at the midpoint of the rod

7 Conclusion

A Finite Volume Meshless Local Petrov Galerkin (FVMLPG) method is developed for structural transient problems. The MLS is used for constructing the shape functions at the scattered points. Using with the Newmark scheme for time integration, a numerical treatment is developed for the enforcement of the kinematic boundary conditions, which is very effective, computationally. The numerical examples show the capability of the present FVMLPG method for simulating both the transient structural responses. It can be concluded that the present FVMLPG method has many distinct advantages.

References

[1] Atluri S. N., Zhu T., A new meshless local Petrov-Galerkin (MLPG) approach in computational mechanics. Computational Mechanics, 1998; 22: 117-127.

[2] Nayroles B., Touzot G., Villon P., Generalizing the finite element method: diffuse approximation and diffuse elements. Computational Mechanics, 1992; 10: 307-318.

[3] Belytschko T., Lu Y. Y., Gu L., Element-free Galerkin methods. Int. J. Numer Methods Engrg. 1994; 37: 229-256.

[4] Liu W. K., Jun S., Zhang Y. F., Reproducing kernel particle methods for structural dynamics. Int. J. Numer. Methods Engrg. 1995; 38: 1655-1679.

[5] Sladek J., Sladek V., Keer R. V., Meshless Local Boundary Integral Equation Method for 2D Elastodynamic Problems. Int. J. Numer. Methods Engrng. 2003; 57: 235-249.

[6] Moosavi M.R., Khelil A., Accuracy and Computational Efficiency of the Finite Volume Method Combined with the Meshless Local Petrov-Galerkin in Comparison with the Finite Element Method in Elasto-static Problem, *ICCES*, Vol. 113, no. 1, pp. 1-28, 2008.

[7] Newmark N. M., A method of computation for structural dynamics, Journal of the Engineering Mechanics Division, ASCE, 1959; 85: 67-94.

[8] Clough R. W., Penzien J., Dynamics of Structures, New York McGraw-Hill, 1975.